REGULAR ARTICLE

Role of chondroitin sulfate in the developmental and healing process of the dental pulp in mice

Hiroko Ida-Yonemochi[1] · Kosei Takeuchi[2] · Hayato Ohshima[1]

Abstract

Chondroitin sulfate proteoglycan (CSPG), one of the major extracellular matrices, plays an important part in organogenesis. Its core protein and chondroitin sulfate (CS) chain have a specific biological function. To elucidate the role of CS in the developmental and healing process of the dental pulp, we performed an experimental tooth replantation in CS N-acethylgalactosaminyltransferase-1 (T1) gene knockout (KO) mice. We also performed cell proliferation assay and qRT-PCR analysis for the WT and T1KO primary dental pulp cells using T1-siRNA technique and external CS. During tooth development, CS was diffusely expressed in the dental papilla, and with dental pulp maturation, CS disappeared from the differentiated areas, including the odontoblasts. In fully developed molars, CS was restricted to the root apex region colocalizing with Gli1-positive cells. In the healing process after tooth replantation, CD31-positive cells accumulated in the CS-positive stroma in WT molars. In T1KO molars, the appearance of Ki67- and Gli1-positive cells in the dental pulp was significantly fewer than in WT molars in the early healing stage, and collagen I-positive reparative dentin formation was not obvious in T1KO mice. In primary culture experiments, siRNA knockdown of T1 gene significantly suppressed cell proliferation in WT dental pulp cells, and the mRNA expression of *cyclin D1* and *CD31* was significantly upregulated by external CS in T1KO dental pulp cells. These results suggest that CS is involved in the cell proliferation and functional differentiation of dental pulp constituent cells, including vascular cells, in the healing process of dental pulp tissue after tooth injury.

Keywords Chondroitin sulfate · Heparan sulfate · Dental pulp · Tooth replantation · Vessels

Introduction

Glycosaminoglycans (GAGs), the major carbohydrate component of proteoglycans (PGs), play an important part in controlling cell kinetics in the pathophysiological situations.

✉ Hiroko Ida-Yonemochi
hyone@dent.niigata-u.ac.jp

1 Division of Anatomy and Cell Biology of the Hard Tissue, Department of Tissue Regeneration and Reconstruction, Niigata University Graduate School of Medical and Dental Sciences, 2-5274 Gakkocho-dori, Chuo-ku, Niigata 951-8514, Japan

2 Department of Medical Cell Biology, Medical Research Creation Center, Aichi Medical University, Nagakute, Aichi 480-1195, Japan

Chondroitin sulfate (CS) is one of the major GAGs containing N-acetylgalactosamine (GalNAc) and glucuronic acid (GlcA), and regulates cell behavior by interacting with signaling molecules, such as Wnts, hedgehog, and fibroblast growth factors (FGFs) (Nadanaka et al. 2011; Prinz et al. 2014; Mizumoto et al. 2015). CS is abundantly distributed in the brain and cartilage, and is known to inhibit axonal growth and chondrocyte apoptosis, whereas heparan sulfate (HS) is composed of N-acetylglucosamine (GlcNAc) and GlcA, and has many biological functions, such as axonal growth promotion and angiogenesis, by modulating the growth factors, such as the transforming growth factor (TGF)-ß and FGF (Zhang et al. 2019).

During tooth development, PGs abundantly exist in the dental epithelial and mesenchymal tissues, and modulate tooth morphogenesis and organization (Ida-Yonemochi et al. 2005; Listik et al. 2019; Randilini et al. 2020). In the dental pulp tissue, a

chondroitin sulfate proteoglycan (CSPG), versican, is present in the subodontoblastic region of the rat molar dental pulp (Shibata et al. 1999, 2002), and the inhibition of CSPG incorporation to the odontoblasts by ß-xyloside disturbs odontoblast differentiation of embryonic mouse molars in vitro (Liu et al. 2017). In addition, NG2, one of the major CSPGs, is located on the cell surface of perivascular cells in the dental pulp, and NG2-positive cells have been shown to differentiate into odontoblasts (Yang et al. 2019). On the other hand, HS is located along the blood vessels in the dental pulp (Ida-Yonemochi et al. 2010); a cell surface HSPG, glypican-1, is known to be associated with early differentiation of odontoblasts (Murakami Masuda et al. 2010). Therefore, PGs are essential for odontoblast differentiation in normal dentinogenesis.

The dental pulp tissue contains a number of cell types, such as odontoblast-lineage cells, immune cells, neurovascular cells, and dental pulp stem cells. PGs regulate the dynamics of these cells, and the core protein and GAG chain each has a biological function for the differentiation and regeneration of dental pulp constituent cells. In particular, CS is known to regulate neurovascular formation, collagen fibrinogenesis, and stem cell behavior in other organs (Prinz et al. 2014; Wang and Yang 2017; Galindo et al. 2018; Wood et al. 2018), whereas HS works indirectly as the binding reservoir for soluble signaling factors. Therefore, we speculate that CS is one of the key molecules that regulate dental pulp organization in the development and regeneration, differently from HS. However, there have been no reports that demonstrate the role of CS in the healing process of the dental pulp comparing with HS.

We have previously proven that CS plays important roles in connective tissue organization and intramembranous ossification of the craniofacial skeleton using CS *N*-acetylgalactosaminyltransferase-1 gene knockout (T1KO) mice (Ida-Yonemochi et al. 2018). CS T1 is a key glycosyltransferase in CS biosynthesis and exhibits GalNAc transfer activity in both the initiation and elongation processes (Uyama et al. 2002; Uyama et al. 2003; Igarashi et al. 2018). In the T1KO mice, the amount of CS was reduced into half compared with wild-type mice (Watanabe et al. 2010). The cartilage of long bone was small with abnormal aggregation of type II collagen fibers (Watanabe et al. 2010), and axonal growth was promoted after the spinal cord injury in T1KO mice (Takeuchi et al. 2013). In the craniofacial region, the shape of the skull changed due to impaired intramembranous ossification and cartilage deformation (Ida-Yonemochi et al. 2018); however, tooth morphogenesis in T1KO mice has not been studied yet.

In this study, we examined the role of CS in normal tooth morphogenesis and healing process by focusing on the dental pulp organization in T1KO mice. We demonstrated that the CS chain was involved in cell proliferation and angiogenesis in the healing process of dental pulp, and supports the functional differentiation of odontoblast and dentin formation during odontogenesis.

Materials and methods

Mice

All the animal experiments were conducted in compliance with the protocol, which was reviewed by the Institutional Animal Care and Use Committee, and were approved by the President of Niigata University (Permit Number: #28 Niigata Univ. Res. 42–9). *Csgalnact1* (ID: 234356) knockout (T1KO) mice were derived from the C57BL/6 N strain, and were genotyped and maintained as described previously (Watanabe et al. 2010). Homozygous mutant mice and control mice were obtained by crossing heterozygous pairs. To examine the changes in the tooth morphogenesis in T1KO mice, embryonic days 15.5 and 18.5, and postnatal days 1, 7, 28, and 26 weeks of WT and T1KO mice were used (WT: n = 26, T1KO: n = 26).

Tooth replantation experiment

The upper right and left first molars of three-week-old WT and T1KO mice were extracted with a pair of dental tweezers and then repositioned in its original socket immediately (Saito and Ohshima 2017). This procedure was performed under deep anesthesia, which consisted of an intraperitoneal injection of chloral hydrate (maximum dose of 350 mg/kg). The alveolar sockets were not treated after extractions, and no additional treatments, such as the fixation of teeth or relief of occlusion, were performed following tooth replantation. After 3, 5, 7, and 14 days, the mice were fixed as described below (WT: n = 12, T1KO: n = 12).

Histology

The mice were perfused with physiological saline, followed by 4% paraformaldehyde in a 0.1 M phosphate buffer (pH 7.4). The maxillae were removed en bloc and decalcified in a 10% ethylenediamine tetraacetic acid disodium salt (EDTA-Na$_2$) solution for two weeks at 4 °C. Then, the samples were embedded into paraffin, and serial sections (4 μm) were cut, stained with hematoxylin and eosin (HE), azocarmine and aniline blue (Azan), and processed for immunohistochemistry using the antibodies described below.

Immunohistochemistry

Immunohistochemistry was performed according to our previous report (Ida-Yonemochi et al. 2016) with a mouse anti-chondroitin sulfate A (CS-A) monoclonal antibody diluted to 1:500 (Seikagaku biobusiness corp. Tokyo, Japan; catalog number: 370710), a mouse anti-chondroitin sulfate monoclonal antibody diluted to 1:400 (clone CS-56, Sigma-Aldrich Co., St. Louis, MO, USA; catalog number: SAB4200696), a mouse anti-HS monoclonal antibody diluted to 1:100 (Seikagaku biobusiness corp.; catalog number: 370255), a mouse anti-nestin monoclonal antibody diluted to 1:100 (EMD Millipore, Billerica, MA, USA; catalog number: MAB353), a rabbit anti-versican monoclonal antibody diluted to 1:100 (Abcam, Cambridge, UK; catalog number: 177480), rabbit anti-aggrecan polyclonal antibody diluted to 1:100 (Abcam; catalog number: 36861), rabbit anti-Gli1 polyclonal antibody diluted to 1:500 (Novus Biologicals, Littleton, CO, USA; catalog number: NBP1-78,259), rabbit anti-collagen type I polyclonal antibody diluted to 1:250 (Abcam; catalog number ab21286), rabbit anti-PGP9.5 polyclonal antibody diluted to 1:2500 (Proteintech Japan, Tokyo, Japan; catalog number: 14730–1-AP), rat anti-CD31 monoclonal antibody diluted to 1:50 (BD Pharmingen, USA; catalog number: 553370), and rat anti-Ki67 monoclonal antibody diluted to 1:100 (Dako, Glostrup, Denmark; catalog number: M7249). The antigens were exposed by autoclaving the samples in citric acid buffer (pH 6.0) at 121 ℃ for 5 min for Gli1 and Ki67, 0.1% trypsin (Sigma) in 0.01 M Tris–HCl at 37 ℃ for 15 min for CD31 or 3 mg/mL bovine testicular hyaluronidase (type I-S, 440 U/mg, Sigma) in PBS for 30 min at 37℃ for HS, versican and aggrecan. Then, the sections were treated with 0.3% hydrogen peroxide in methanol for 30 min at room temperature to block endogenous peroxidase activity. Next, the samples were incubated overnight at 4℃ with primary antibodies diluted in T-PBS. The Envision detection system (peroxidase/DAB, rabbit/mouse) (Dako Japan; catalog number: K5027) or the avidin–biotin peroxidase complex (ABC) (Vectastain ABC kit; Vector Laboratories, Burlingame, CA, USA) method using biotinylated anti-rat IgG (Vector Laboratories; catalog number: BA-4000) diluted to 1:100 or anti-rabbit IgG (Vector Laboratory; BA-1000) diluted to 1:200 was used. To visualize the reaction products, the sections were treated with 0.02% 3,3′-diaminobenzidine (Dohjin Laboratories, Kumamoto, Japan) in 0.05 M Tris–HCl buffer (pH 7.4) containing 0.005% hydrogen peroxide and were counterstained with hematoxylin. For the negative control staining, the primary antibodies were replaced with PBS, showing no specific immunoreaction.

For double immunofluorescent staining, the paraffin sections were treated with Texas Red-conjugated anti-mouse IgG + IgM (diluted to 1:500; Rockland, Gilbertsville, PA, USA), FITC-conjugated anti-rabbit IgG (diluted to 1:500; Vector Laboratories, Burlingame, CA, USA), or FITC-conjugated streptavidin (diluted to 1:250; Vector Laboratories). The stained sections were analyzed with a confocal laser scanning microscope (FV300, Olympus, Tokyo, Japan).

Analysis using Image J software on the tissue sections

The thickness of predentin matrix in WT and T1KO molars was measured on the tissue sections by Image J software (National Institute of Health, Bethesda, MD, USA). Each three HE-stained sections of frontal plane crossing the center of maxillary first molars were taken photographs with the scale on the microscope. The thickness of predentin in the crown was measured in three areas from each photograph by straight line tool of Image J (Fig. S1a), and their average length was used for statistical analysis. The straight line tool of Image J was set along the dentinal tubules. For measurement of collagen 1-positive area in predentin, we measured the whole predentin area in the sections of frontal plane crossing the center of maxillary first molars. The area selection tool of Image J was used in the collagen I-immunostained sections (Fig. S1b). In addition, the nestin- and collagen 1-positive perimeters in the whole internal surface of predentin were measured with the freehand tool of Image J (Fig. S1c).

Analysis by electron probe micro analyzer (EPMA)

Sagittal-cutting mandibular incisors and molars were analyzed by EPMA (EPMA-8705, Shimadzu, Kyoto, Japan) to detect chemical elements. The mandibles were fixed with 4% PFA, rinsed with 0.1 M cacodylate buffer (pH 7.4), dehydrated with an ascending series of acetone, and embedded in Epon 812 (Taab, Berkshire, UK). The samples were ground down to detect calcium, magnesium, and phosphorus by EPMA (EPMA-8705, Shimadzu, Kyoto, Japan). The common voltage and electrical current settings were 15.0 kV and 0.025 µA, respectively. The obtained data of the point measurements were transferred into various colors according to the concentration of the mineral.

Table 1 The primers used for quantitative real-time PCR analysis

Molecule	Primer sequence	Amplicon size	Entrez Gene ID
β-actin			
Forward	5'- GTGGGAATGGGTCAGAAGGA -3'	120 bp	NM 007,393
Reverse	5'- CTTCTCCATGTCGTCCCAGT -3'		
Nanog			
Forward	5'- TGTGTGCACTCAAGGACAGGTT -3'	85 bp	AY278951
Reverse	5'- TCAGGTTCAGAATGGAGGAGAGTT -3'		
Nestin			
Forward	5'- GACCAGGTGCTTGAGAGACT -3'	140 bp	BC062893
Reverse	5'- ACCTGGTCCTCTGCTTCTTC -3'		
CyclinD1			
Forward	5'- GCGTACCCTGACACCAATCT -3'	329 bp	NM 007,631
Reverse	5'- CACAACTTCTCGGCAGTCAA -3'		
Collagen 1			
Forward	5'- CACCCTCAAGAGCCTGAGTC -3'	253 bp	NM 007,742
Reverse	5'- GTTCGGGCTGATGTACCAGT -3'		
Integrin β1			
Forward	5'- GCCAGGGCTGGTTATACAGA -3'	226 bp	MN010578.1
Reverse	5'- TCACAATGGCACACAGGTTT -3'		
CD31			
Forward	5'- AGTCAGAGTCTTCCTTGCCC -3'	125 bp	NM 008,816
Reverse	5'- TCTGTTTGGCCTTGGCTTTC -3'		
PGP9.5			
Forward	5'- CACAGCTGTCTTCTTGCGTT -3'	120 bp	NM 011,670
Reverse	5'- AGCAAGGTACGAGACACACA -3'		

Primary culture of dental pulp cells

The mandibular first molars of 3-week-old WT and T1KO mice were dissected, and the dental pulp tissues were separated manually under a stereomicroscope. They were incubated with 2% collagenase/α-MEM solution for 30 min at 37 ℃ to dissociate the dental pulp cells. The suspended dental pulp cells were plated into 35-mm plastic dishes in 2 ml of α-MEM (Gibco BRL, Grand Island, NY, USA) with 10% fetal bovine serum and 1% penicillin–streptomycin. They were incubated at 37℃ under a humidified 5% CO_2/95% air atmosphere. When the cells became confluent, they were split again and used for the experiments described below.

Small interfering RNA experiment

Small interfering RNA (siRNA) transfection to primary dental pulp cells was performed using Lipofectamine ™ RNAiMAX (Invitrogen). Control siRNA (20 nM, sc-37007, Santa Cruz,) or *T1* siRNA (20 nM, GCAAUCAAAGGC UAUGAAUGA) was applied to the cells for 48 h.

Cell proliferation assay

The cells were plated in 96-well plates at a density of 2×10^3 cells/well. To each well, 10 μL of the Cell Counting Kit-8 (CCK-8, Dohjin Laboratories, Kumamoto, Japan)

Fig. 1 Expression of CS and HS during mouse molar development. Immu-▶ nohistochemical staining for CS-A and HS in the maxillary first molar at E13.5 (**a**, **d**), E15.5 (**b**, **e**), E18.5 (**c**, **f**), P3 (**g**, **j**), and P28 (**h**, **i**, **k**, **l**). Double immunofluorescent staining of CS-A/Gli1 (**m**), CS-A/PGP9.5 (**n**), and CS-A/CD31 (**o**) (**a**) CS is not obvious in the dental mesenchyme at E13.5. (**b**, **c**) After E15.5, CS is strongly expressed in the dental papilla. (**d**) HS is strongly localized in the condensed dental mesenchymal tissue at E13.5. (**e**, **f**) HS dramatically disappears from the dental papilla, and is restricted in the basement membrane. (**g**) CS disappears from the dental pulp with maturation and remained in the subodontoblastic layer at P3. (**h**) At P28, CS is strongly immunolocalized only in the apex region of tooth root. (**i**) Higher magnification of the boxed area in **h**. (**j**) HS is restricted in the substratum area of mature odontoblasts at P3. (**k**) At P28, HS is diffusely immunopositive in the whole dental pulp. (**l**) Higher magnification of the boxed area in **k**. (**m**) Gli1-positive cells (green) are densely localized in CS-positive area (red). (**n**) PGP9.5-positive neurons (green) are colocalized with CS. (**o**) CD31-positive vessels (green) are present along with the CS-positive matrix. *dp*; dental pulp. Bars, 100 μm (**a–c**, **i**); 250 μm (**g**); 500 μm (**h**)
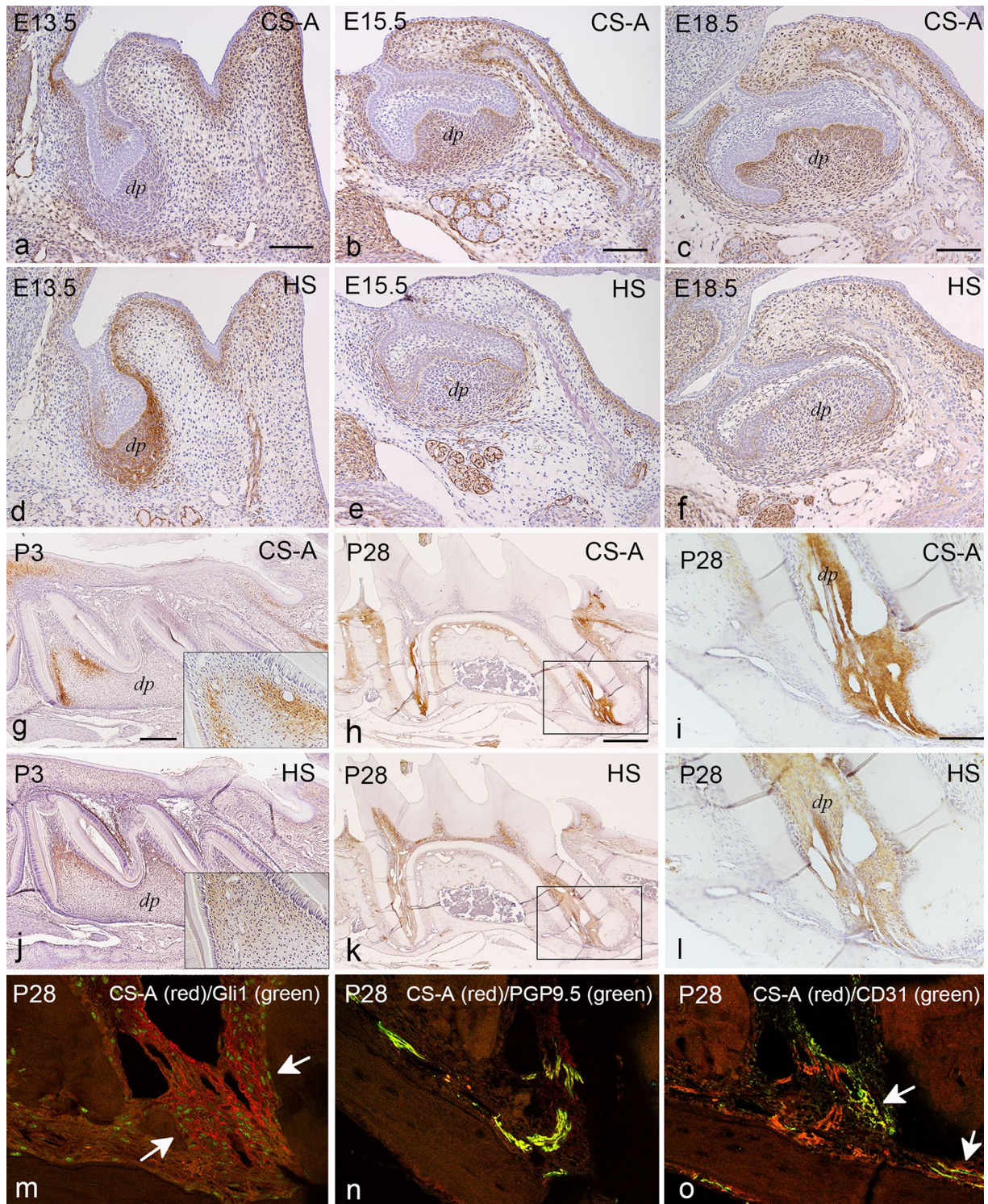
Corp., Wisconsin, USA) at a wavelength of 450 nm. The experiment was repeated three times to confirm the results.
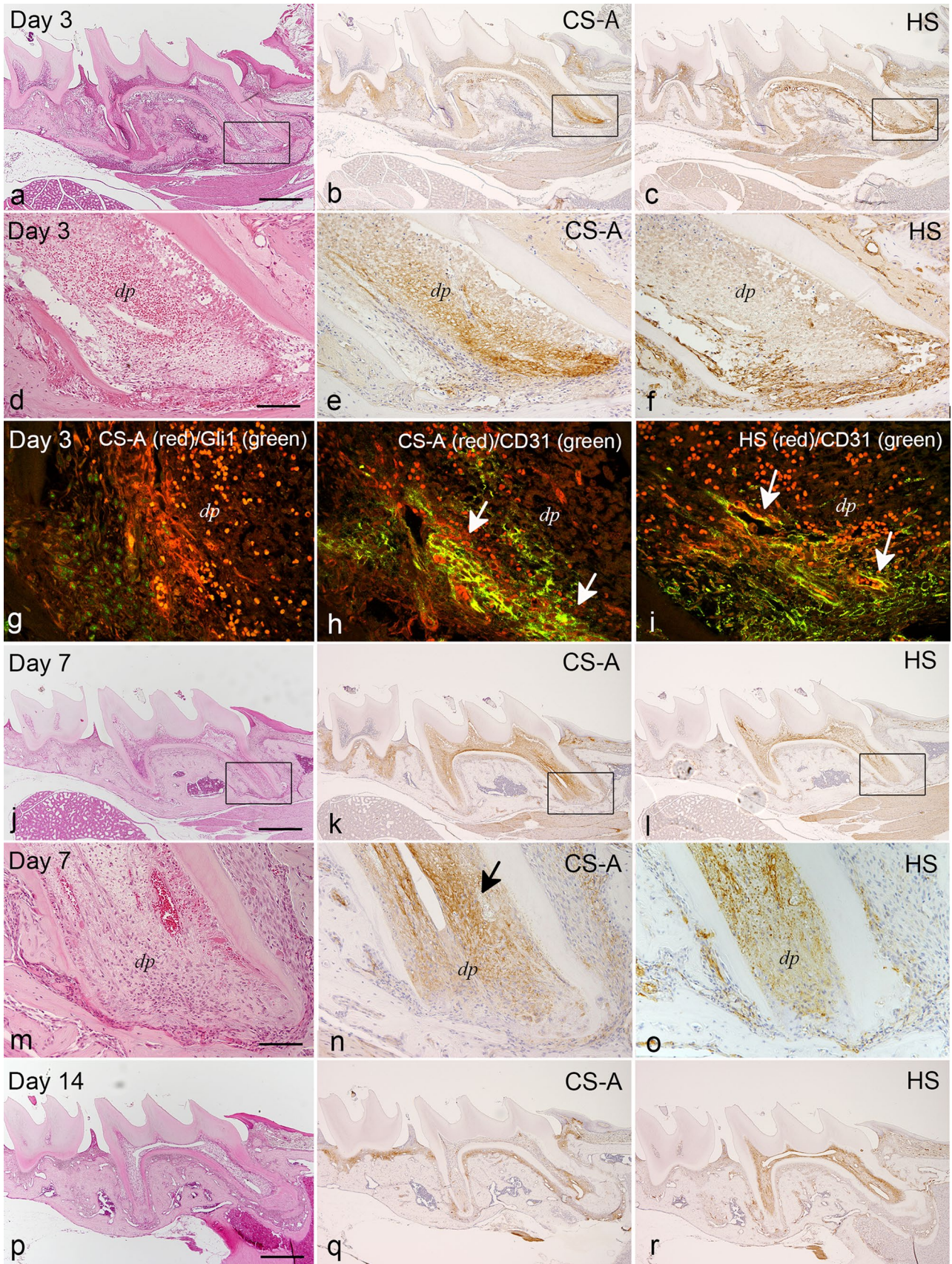
◄**Fig. 2** Changes in CS/HS distribution in the healing process of dental pulp tissue. HE (**a**, **d**, **j**, **m**, **p**) and immunohistochemical staining for CS-A (**b**, **e**, **k**, **n**, **q**) and HS (**c**, **f**, **l**, **o**, **r**). (**a**, **b**) CS-A is weakly immunopositive in the whole dental pulp, and the strong immunoreactivity of CS is observed in the apical papilla after three days. (**c**) HS shows the opposite expression pattern of CS, surrounding the CS-positive apical papilla. (**d**–**f**) Higher magnification of the boxed area in **a**–**c**. (**g**) Gli1-positive cells (green) are located beside the dense CS-positive area (red) in the root apex after three days. (**h**) CD31-positive cells colocalize with CS (arrows). (**i**) Tubularly formed vessels are colocalized with HS, not CS (arrows). (**j**–**o**) The immunopositivity of CS and HS is enhanced in the whole dental pulp tissue after seven days, and the strong immunoreaction of CS shifts from the apical papilla to the crown side, as indicated by arrow (**n**). (**m**, **n**, **o**) Higher magnification of the boxed area in **j**–**l**. (**p**–**r**) At day 14, the distribution of CS and HS is the same as that of normally developed molar shown in Fig. 1. CS is restricted in the apex region of the root pulp (**q**). *dp*, dental pulp. Bars, 500 μm (**a**, **j**, **p**); 100 μm (**d**, **m**)

Quantitative real-time PCR analysis

The cells were plated in 12-well plates with or without CS-A coat (50 μg/mL, Sigma, catalog number: C9819) at a density of 1×10^4 cells/well. After 48 h, the total RNA was isolated using the Trizol system (Invitrogen, Carlsbad, CA, USA). cDNA was synthesized using the Prime Script 1st strand cDNA Synthesis Kit (Takara, Otsu, Japan). Real-time PCR was performed using SYBR1 Premix Ex Taq II (Takara) and oligonucleotide primers specific for the target sequences (Table 1) on a Thermal Cycler Dice (Takara). The amplification conditions were as follows: 30 s at 95 ℃; 50 cycles of 95 ℃ for 5 s, and 60 ℃ for 30 s; dissociation for 15 s at 95 ℃; and 30 s at 60 ℃. The relative gene expression levels were calculated relative to the levels of ß-actin mRNA using the 2nd Derivative Maximum (2−ΔΔCt) method. The experiment was repeated three times to confirm the results.

Statistical analysis

All data are presented as the means and standard errors of each group. StatPlus for Mac (AnalystSoft Inc., Vancouver, BC, Canada) was used to perform the statistical analyses. Student's *t* test assuming equal variances was used for single comparison.

Results

Contrasting expression of CS and HS in dental mesenchyme during tooth development

To demonstrate the expression patterns of CS compared with HS in dental pulp development, we observed the first maxillary molar at different developmental stages.

Throughout all developmental stages, the opposite expression between CS and HS was observed (Fig. 1). To detect CS expression, we used two kinds of antibodies, CS-A (clone: 2H6) and CS (clone: CS-56), and they showed nearly the same staining patterns (Figs. 1, S2). At embryonic day 13.5 (E13.5), CS was not obvious in the dental mesenchyme (Figs. 1a, S2a), while HS was strongly localized in the condensed dental mesenchymal tissue (Fig. 1d). After E15.5, CS was diffusely expressed in the dental papilla and dental follicular tissue (Figs. 1b, S2d), and it was strongly detected beneath the basement membrane facing to the inner enamel epithelium at E18.5 (Figs. 1c, S2g). On the other hand, HS dramatically disappeared from dental papilla, and it was restricted in the basement membrane at E15.5 and E18.5 (Fig. 1e, f).

With the maturation of dental pulp tissue, CS disappeared from the majority of dental pulp and remained in the subodontoblastic layer at P3 (Figs. 1g, S2j). In contrast, HS reappeared in the dental pulp and was restricted in the substratum area of mature odontoblasts (Fig. 1j). In the fully developed molar at P28, CS was strongly immunolocalized in the apex region of the tooth root and the periodontal ligament, although it was completely disappeared from the coronal pulp (Figs. 1h, i, S2m, p). On the other hand, HS was diffusely immunopositive in the dental pulp of both tooth crown and root (Fig. 1k, l). To examine the relationship between CS and stem cell/nerve/blood vessel distributions in the dental pulp, we performed double immunofluorescent staining for their specific markers. Gli1-positive cells were densely localized in the CS-positive area (arrows, Fig. 1m), and PGP9.5-positive neurons were colocalized with CS in the root apex area (Fig. 1n). CD31-positive vessels were present along with CS-positive matrix (arrows, Fig. 1o). To compare the expression of CS chain with its core protein, we performed immunostaining for versican and aggrecan together with CS (Fig. S2). Versican core protein coexisted with CS in the dental pulp, not aggrecan (Fig. S2b, e, h, k, n, q). Aggrecan appeared in the apical papilla region and periodontal ligament of developed molars (Fig. S2o, r). The results of negative control staining are shown in Fig. S3.

Changes in CS/HS distribution in the healing process of dental pulp

To observe the healing process of dental pulp, we performed tooth replantation experiment of maxillary first molar in 3-week-old mice. Three days after replantation, CS was weakly immunopositive in the whole dental pulp (Figs. 2a, b, S4a), and the strong immunoreactivity of CS was observed in the apical papilla (Figs. 2d, e, S4d). HS showed the opposite expression pattern with CS,
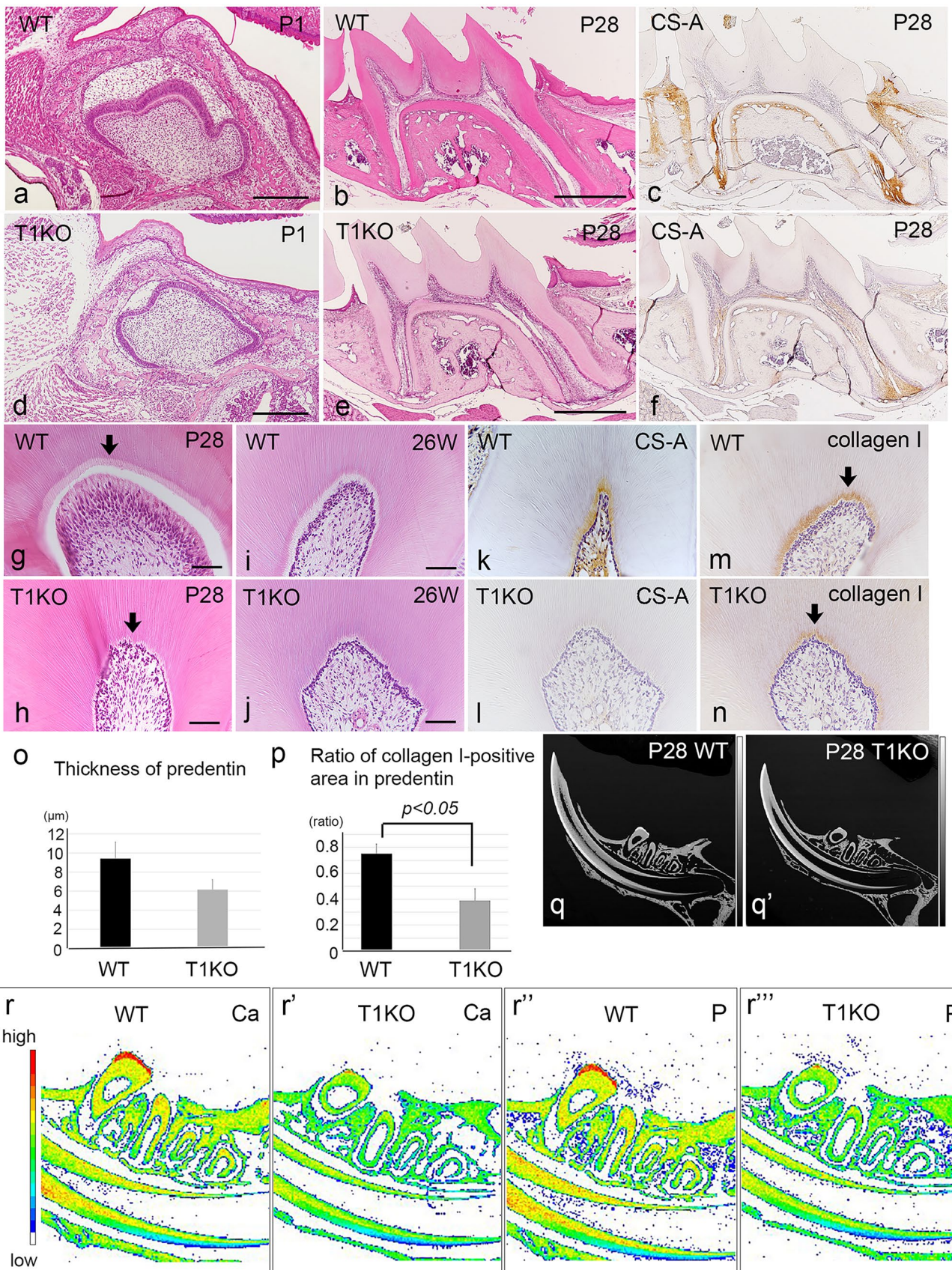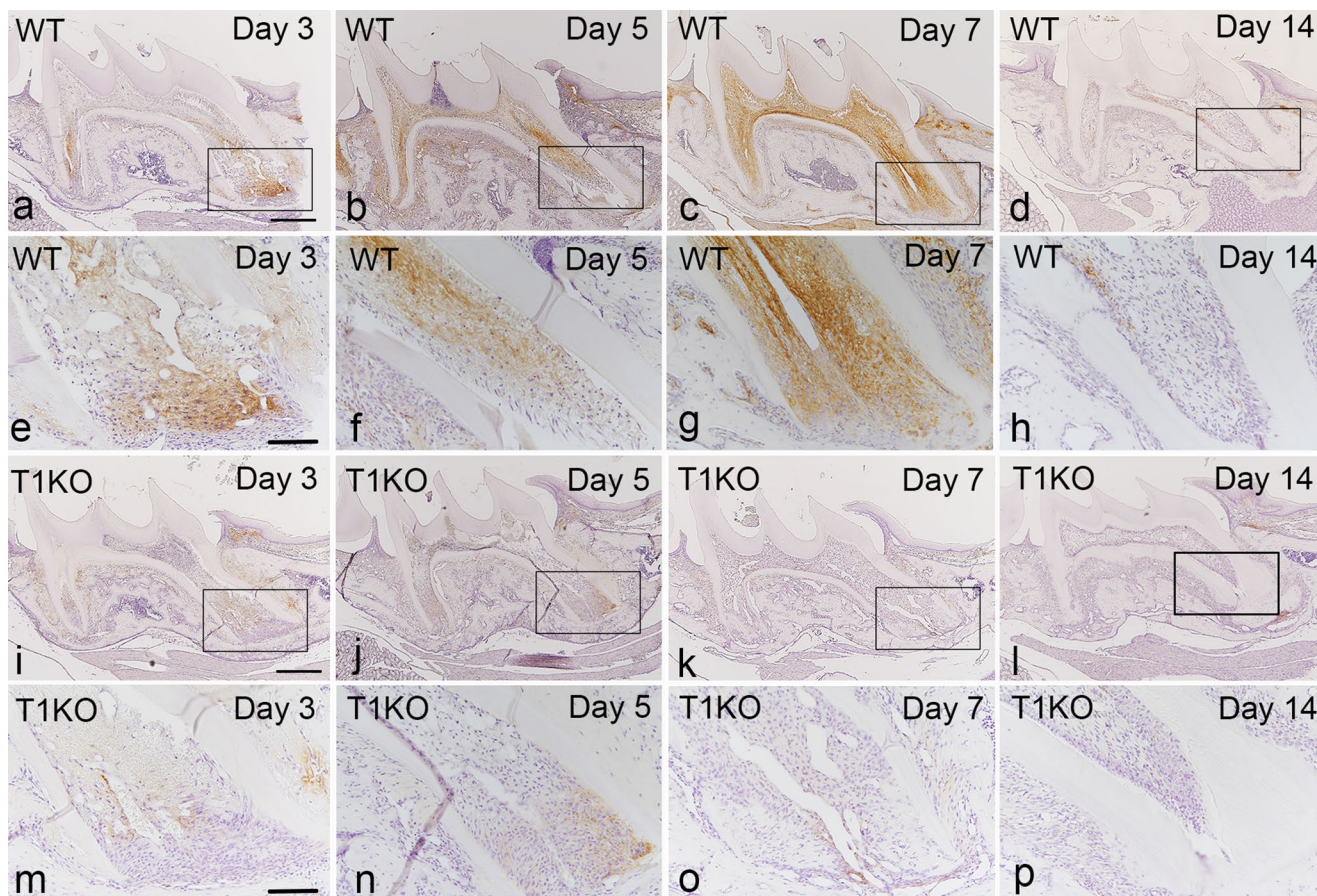
◀**Fig. 3** Developmental features of maxillary molars in T1KO mice. HE (**a, b, d, e, g, i, h, j**), immunohistochemical staining for CS-A (**c, f, k, l**) and collagen type I (**m, n**). EPMA analysis of the mandible (**q-r'''**). (**a–f**) Histologically, there are no obvious differences in the early molar morphogenesis between WT and T1KO mice. The expression of CS is less in T1KO dental pulp than WT dental pulp (**c, f**). (**g–o**) The predentin is thin and irregular in the T1KO molars of adult mice (arrows in **g, h**). (**m, n, p**) The deposition of collagen 1 in the predentin significantly reduces in T1KO molars (arrows in **m, n**). (**q, q'**) Backscattered electron image of the mandible at P28. (**r-r'''**) The amounts of Ca and P tend to decrease in the T1KO molars. n = 4 for each, Student's *t* test (**o, p**). Bars, 250 µm (**a, d**); 500 µm (**b, e**); 50 µm (**g-j**)

surrounding the CS-positive apical papilla (Fig. 2c, f). To confirm the effect of CS on stem cell movement and angiogenesis in the dental pulp, we performed double immunofluorescent staining using their specific markers. Gli1-positive proliferating cells were located beside the dense CS-positive area in the root apex after three

days (Fig. 2g). Although CD31-positive cells colocalized with CS (arrows, Fig. 2h), tubularly formed vessels were colocalized with HS, not CS (arrows, Fig. 2i). At day 7, the immunopositivity of CS and HS was enhanced in the whole dental pulp tissue (Fig. 2j–l), and the strong immunoreaction of CS shifted from the apical papilla to the crown side, as indicated by arrows (Figs. 2m–o, S4g, j). At day 14, the immunolocalization of CS and HS was the same as that of normally developed molar as shown in Fig. 1 (Fig. 2p–r). CS was restricted in the apex region of the tooth root and periodontal ligament (Figs. 2q, S4m) as shown in Fig. 1h. Versican core protein colocalized with CS in the dental pulp just the same as normal odontogenesis shown in Fig. S2 (Fig. S4). Although aggrecan was not present in the dental pulp at day 3 (Fig. S4c, f) differing from CS and versican, it appeared in the dental pulp as well as periodontal ligament at day 7 (Fig. S4i, l). The results of negative control staining are shown in Fig. S5.

Fig. 4 Expression of CS in the healing process of dental pulp tissue in WT and T1KO molars. Immunohistochemical staining for CS-A in WT (**a–h**) and T1KO (**i–p**) maxillary first molars in the healing process of dental pulp. (**e–h, m–p**) Higher magnification of the boxed area in **a–d, i–l**. The expression of CS-A was less in T1KO dental pulp (**i–p**) comparing with WT (**a–h**) in the pulpal healing process (n = 3 for each). Bars, 500 µm (**a, i**); 100 µm (**e, m**)
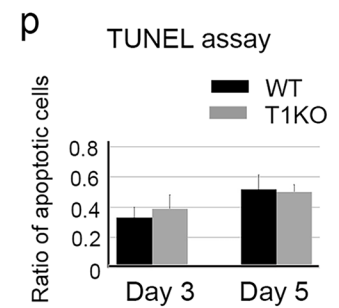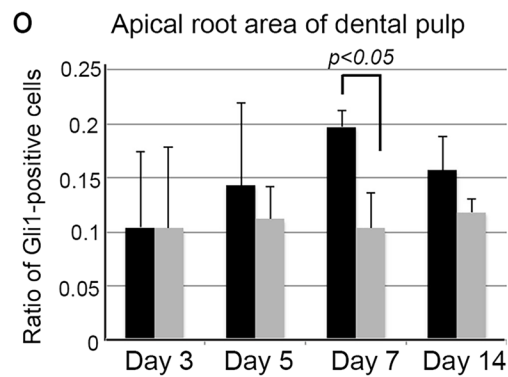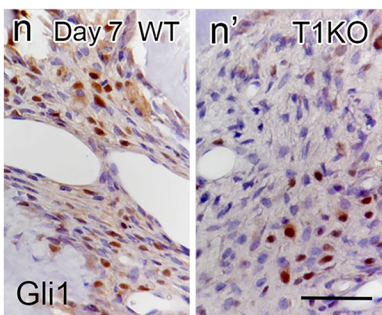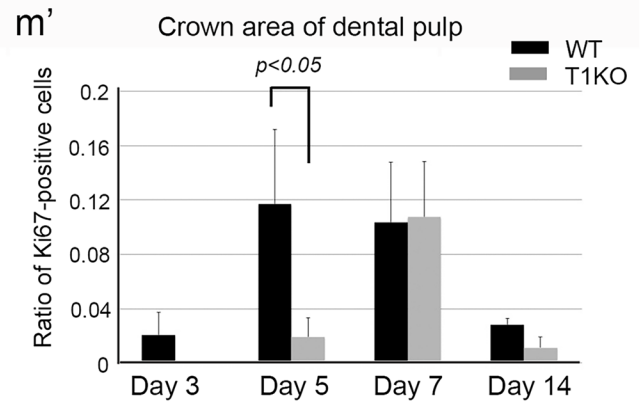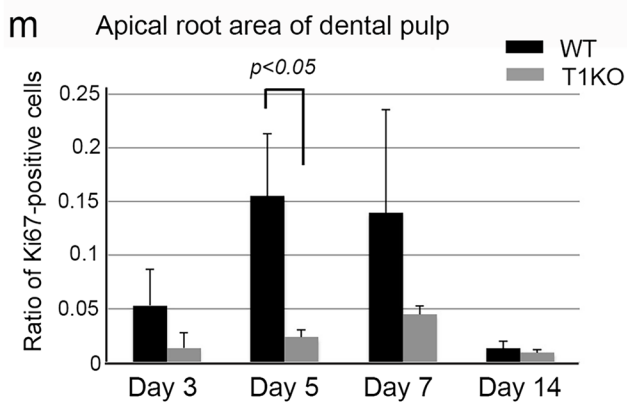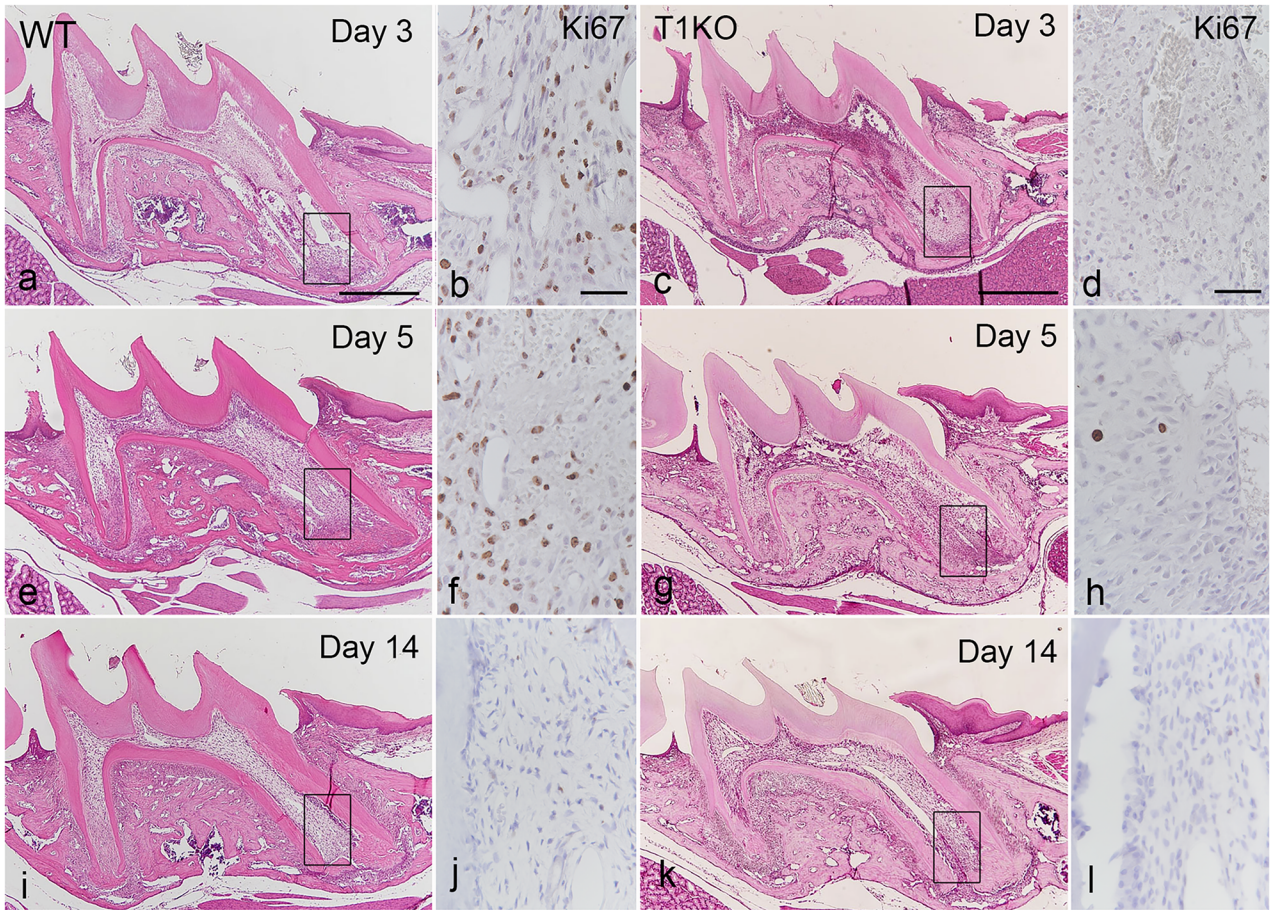
◄**Fig. 5** Pulpal healing process after tooth replantation in T1KO mice. HE (**a, c, e, g, i, k**) and immunohistochemical staining for Ki67 (**b, d, f, h, j, l**) and Gli1 (**n, n'**). (**a–l**) Histologically, the pulpal healing of T1KO molars is similar to that of WT molars until day 14. Cell proliferation is active in the dental pulp especially in the perivascular lesion at days 3 and 5 in WT (**b, f**). However, the appearance of Ki67-positive cells in the T1KO dental pulp is few (**d, h, l**). (**m, m'**) The ratio of Ki67-positive cells is significantly fewer than in WT at day 5. (**n–o**) Gli1-positive cells are also significantly fewer in the root apex region of T1KO dental pulp than in WT at day 7. (**p**) The number of apoptotic cells is not different between WT and T1KO dental pulp cells. n = 3–6 for each, Student's t test (m, o, p). Bars, 500 μm (**a, c**); 50 μm (**b, d, n'**)

Developmental features of maxillary molars in T1KO mice

To examine the influence of CS reduction on tooth formation, we analyzed the chronological changes in maxillary first molar development in T1KO mice. During embryonic and early postnatal stages, there were no obvious differences in tooth morphogenesis between WT and T1KO mice (Fig. 3a, d). At day 28, the shape and size of molars were almost the same with WT and T1KO mice (Fig. 3b, e), although the expression of CS was obviously decreased in T1KO mice than WT mice (Fig. 3c, f). The predentin matrix was thin and irregular in T1KO molars comparing with that of WT molar in adult mice as indicated with arrows (Fig. 3g–o). The deposition of collagen type I in the predentin significantly reduced in T1KO molars (arrows, Fig. 3m, n, p). To observe the influence of dentin calcification on T1KO mice, we checked the mineral density of their mandibular molars using EPMA. We analyzed the exactly same sagittal plane of mandible in WT and T1KO mice (Fig. 3q, q'), and the amounts of Ca and P tended to decrease in the T1KO molars (Fig. 3r-r''').

Reduced cell proliferation in the pulpal healing process in T1KO mice

In the normal developmental and healing process of the dental pulp, CS was strongly immunolocalized in the immature dental papilla/pulp tissues, and was dramatically disappeared with maturation (Figs. 1 and 2). Therefore, we hypothesized that CS might support the differentiation of dental pulp cells and maintain the undifferentiated state of the dental pulp stem cells. To elucidate the role of CS in the healing process of dental pulp, we performed tooth replantation experiment using T1KO mice. Histologically, the pulpal healing of T1KO molars was similar to that of WT molars until day 14 (Figs. 4a–d, i–l, 5a, c, e, g, i, k), although the expression of CS was less in T1KO dental pulp (Fig. 4i–p) comparing with WT (Fig. 4a–h) in the pulpal healing process. We confirmed the immunoreactivity of CS using 3 samples for each condition, and the results were almost the same with Fig. 4. In the WT molars, cell proliferation was active in the dental pulp,

especially in the perivascular lesion at days 3 and 5 (Fig. 5b, f, j). However, the appearance of Ki67-positive cells in the root apex and crown region of T1KO dental pulp was significantly fewer than in WT at day 5 (Fig. 5d, h, l, m, m'). In addition, Gli1-positive cells were significantly fewer in the root apex region of T1KO dental pulp than in WT at day 7 (Fig. 5n, n', o). Between WT and T1KO dental pulp cells, the number of apoptotic cells was not different (Fig. 5p). Next, we checked the odontoblast-like cell differentiation and reparative dentin formation in the healing process. After 7 days of tooth replantation, a few nestin-positive odontoblast-like cells were observed in root area of WT and T1KO molars (Fig. 6a, b), and collagen I-positive reparative dentin was not seen at day 7 (Fig. 6c, d). After 14 days, the differentiation of nestin-positive odontoblast-like cells was observed in both WT and T1KO molars (Fig. 6e, f, i), but the deposition of collagen I in reparative dentin was not obvious in T1KO molars (Fig. 6g, h, j). The reparative dentin matrix was more irregular in T1KO mice than in WT molar (Fig. 6k, k'), and the thickness of reparative dentin, which was bound by osteopontin-positive line, tended to diminish in T1KO molars (Fig. 6k'', k''', l).
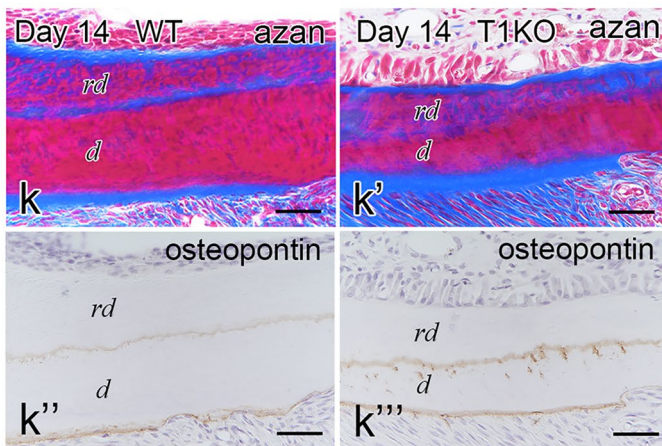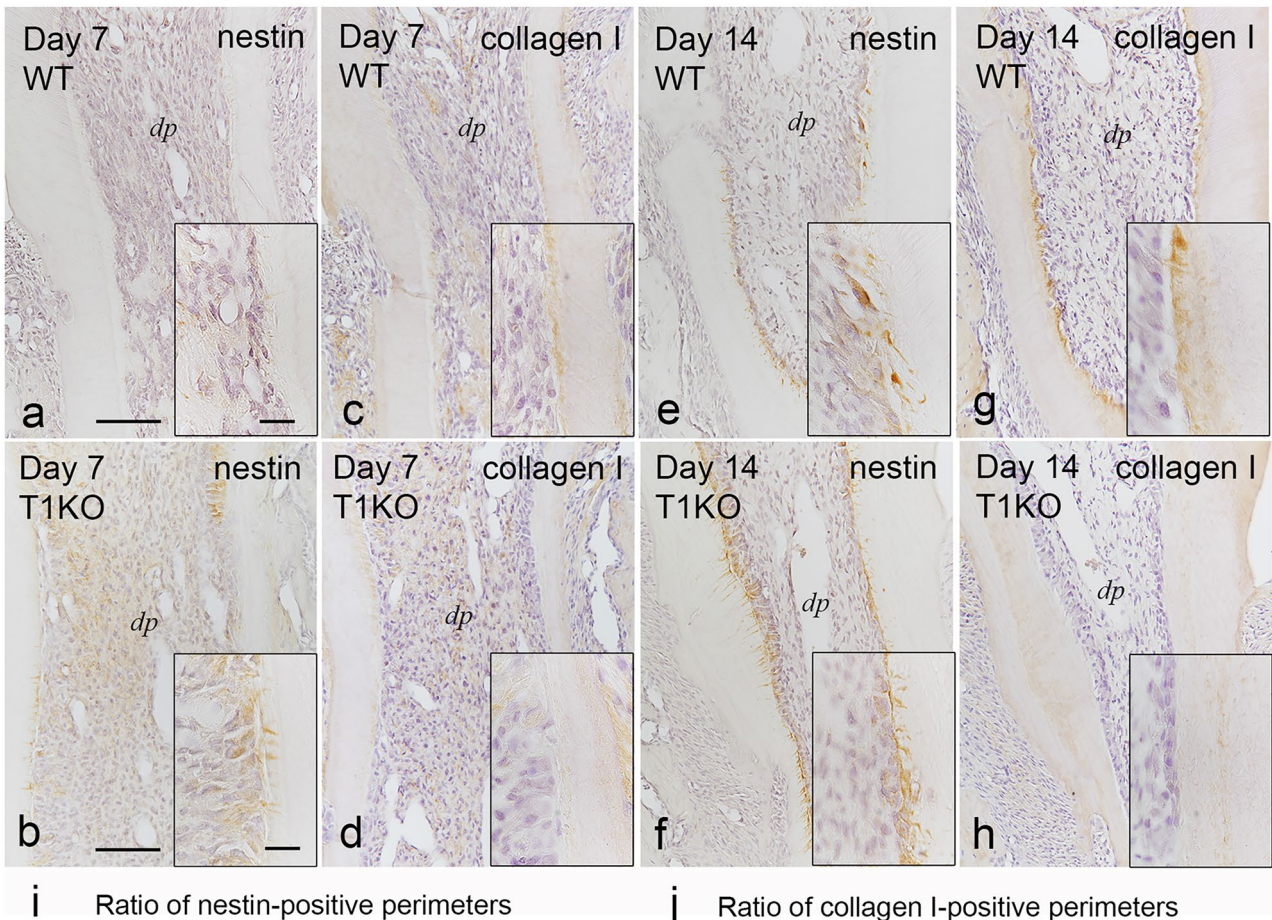
Effect of T1 gene knockdown and extracellular CS on dental pulp cells in vitro

To confirm the effect of absence or presence of CS on dental pulp cells, we performed primary cell culture experiment of WT and T1KO dental pulp cells using T1-siRNA technique or recombinant CS-A. Based on the CCK-8 assay, T1 gene knockdown significantly inhibited cell proliferation of WT dental pulp cells (Fig. 7a). Next, we confirmed the effect of extracellular CS on dental pulp cells. We used T1KO primary dental pulp cells due to exclude the effect of internal CS. The mRNA expression of cell proliferation marker, *cyclin D1*, and endothelial cell marker, *CD31*, was significantly upregulated by extracellular CS in the T1KO cells (Fig. 7b). The stem cell marker, nanog, and odontoblast differentiation markers, such as nestin, DSPP, and collagen 1, were not changed by CS-A for 48 h.

Discussion

This study demonstrated the expression profile of CS in the dental pulp of mouse molars comparing with HS. The role of CS in the healing process of the dental pulp was examined by tooth replantation experiment in T1KO molars. This is the first report to show that CS localizes in the apical papilla region of developed molars, and regulates the proliferation of dental pulp cells and the functional differentiation of odontoblasts in the healing process of the dental pulp.

The extracellular matrix of the dental pulp mainly consists of collagen type I and CSPG, such as versican and biglycan
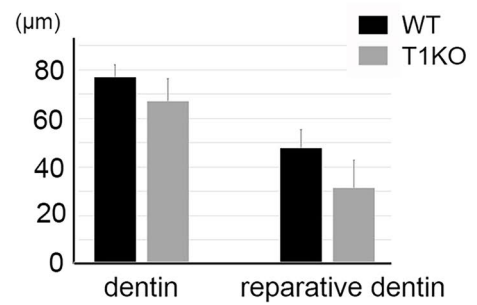
◂**Fig. 6** Odontoblast differentiation and reparative dentin formation in the pulpal healing process in T1KO molars. Immunohistochemical staining for nestin (**a**, **b**, **e**, **f**), collagen I (**c**, **d**, **g**, **h**), and osteopontin (**k**) at days 7 and 14 after tooth replantation, and azan staining (**k,** **k'**) in WT and T1KO molars. (**a**, **b**) A few nestin-positive cells are observed in the root area of T1KO molars. (**c**, **d**) Collagen I-positive reparative dentin is not seen at day 7. (**e**, **f**, **i**) Nestin-positive odontoblasts are observed in the perimeter of dentin in WT and T1KO molars at day 14. (**g**, **h**) The deposition of collagen I-positive newly formed matrix is not observed in T1KO molars. (**j**) The ratio of collagen I-positive perimeters on the surface of reparative dentin is significantly lower in the T1KO mice at day 14. (**k-l**) The reparative dentin matrix is irregular, and the thickness of reparative dentin, which is bound by osteopontin-positive line, tended to diminish in T1KO molars. n = 4–6 for each (**i**), n = 3–4 for each (**j**), n = 4 for each (**l**), Student's t test. *dp*, dental pulp; *d*, dentin; *rd*, reparative dentin. Bars, 100 μm (**a**, **b**); 25 μm (square in **a**, **b**); 50 μm (**k-k'''**)

(Shibata et al. 1999; Listik et al. 2019), maintains tissue homeostasis, and regulates cell kinetics responding to the external stimuli of the dental pulp. A variety of cells exist in the dental pulp, and they are distributed heterogeneously within the pulp tissue. In the human dental pulp, several kinds of stem cells have been isolated such as dental pulp stem cells (DPSCs) (Sui et al. 2020) and stem cells from apical papilla (SCAP) (Sonoyama et al. 2006). They have different characteristics in cell surface markers and differentiation capacities (Lei et al. 2021). In this study, we demonstrated that CS continued to condense in the apical papilla region of fully developed molars, different from HS, and Gli1-positive cells were densely located in the CS-positive area (Fig. 1). In the neural stem cells, CS is reported to maintain stem cells in the neural precursor state (Canning et al. 2016) and impair neural stem cell migration (Galindo et al. 2018). In addition, CS is thought to be a potential modulator of the stem cell niche in the cornea (Ashworth et al. 2020). Therefore, it is speculated that the periapical CS might maintain SCAP as the stem cell niche.

During tooth development, the distribution of CS dramatically changed within the dental papilla/pulp tissue, differing from HS. CS was immunolocalized in the immature dental papilla stroma throughout the developmental stages, and gradually disappeared from differentiated area of coronal pulp (Fig. 1). These changes were also observed in the pulpal healing process after tooth replantation (Fig. 2). Interestingly, CS was temporarily condensed in the subodontoblastic layer at the timing of full odontoblast differentiation (Fig. 1g), which was the same as the versican core protein (Shibata et al. 2002). Subodontoblastic region contains odontoblast progenitor cells with nerve and capillary network (Khadiza et al. 2019). Recent studies demonstrate that the subodontoblastic cell population may differ from odontoblasts in their origin (Nakatomi et al. 2018). Therefore, CS chain might support the differentiation of

odontoblast-lineage cells and neurovascular structure cooperating with growth factors. In the process of neuronal polarization, CS and HS are known to distribute differently and they play opposite functions through regulation of extracellular matrix molecules (Nishimura et al. 2010). As CS stabilizes the growth of axons and HS destabilizes it in an opposing manner (Nishimura et al. 2010), it is speculated that the opposite expression between CS and HS may contribute neurovascular construction in the dental pulp.

In the present study, the immunolocalization of CS is basically the same as versican in the dental pulp. Aggrecan is not obvious in the early stages of developmental and healing process of the dental pulp, but it appears in the apical papilla region and periodontal ligament of developed molars and late stage of pulpal healing. Although the presence of aggrecan in the dental tissue has not been reported yet, we speculate that aggrecan might associate with the maturation of apical papilla and periodontal ligament. Further analyses of the altered expression of CSPG core protein will lead a deeper understanding of the role of CS in the dental pulp.

In the T1KO molars, collagen type I-positive predentin formation was poor, although nestin-positive morphological differentiation was occurred in the odontoblasts during the development and healing process (Figs. 3m, n, 6a–h). Regarding the cause of thinning and irregularity of collagen I-positive predentin matrix in the T1KO molars, the functional maturation of odontoblasts to synthesize collagen I might not be fully occur in the absence of CS. We previously reported that collagen I production was significantly downregulated in T1KO mesenchymal cells, and collagen fibers were irregular and aggregated in the connective tissues in the craniofacial region of T1KO mice (Ida-Yonemochi et al. 2018). Therefore, the same situation might happen in the odontoblasts and predentin matrix in the T1KO molars. In addition, dentin hypomineralization was observed in the T1KO molars (Fig. 3r-r'''). Dorvee et al. have reported that the areas of hypercalcification in dentin contained sulfated CS in bovine (Dorvee et al. 2016), and external CS is known to promote dentin calcification in vitro (Bouvier et al. 1990). Although we could not make clear the exact reason for hypocalcification in T1KO molars, one possibility is that the disorder in collagen I deposition and fibrogenesis with reduced CS might affect dentin matrix formation and calcification. Because it is thought that at the time of mineralization of predentin to dentin, PG and GAG facilitate the organization of the extracellular matrix for mineralization by regulating collagen fibrogenesis (Embery et al. 2001). Since T1KO mice have half the amount of CS, further analyses of dentin–pulp complex by the complete CS knockout mouse model such as T1/T2 double knockout mice (Shimbo
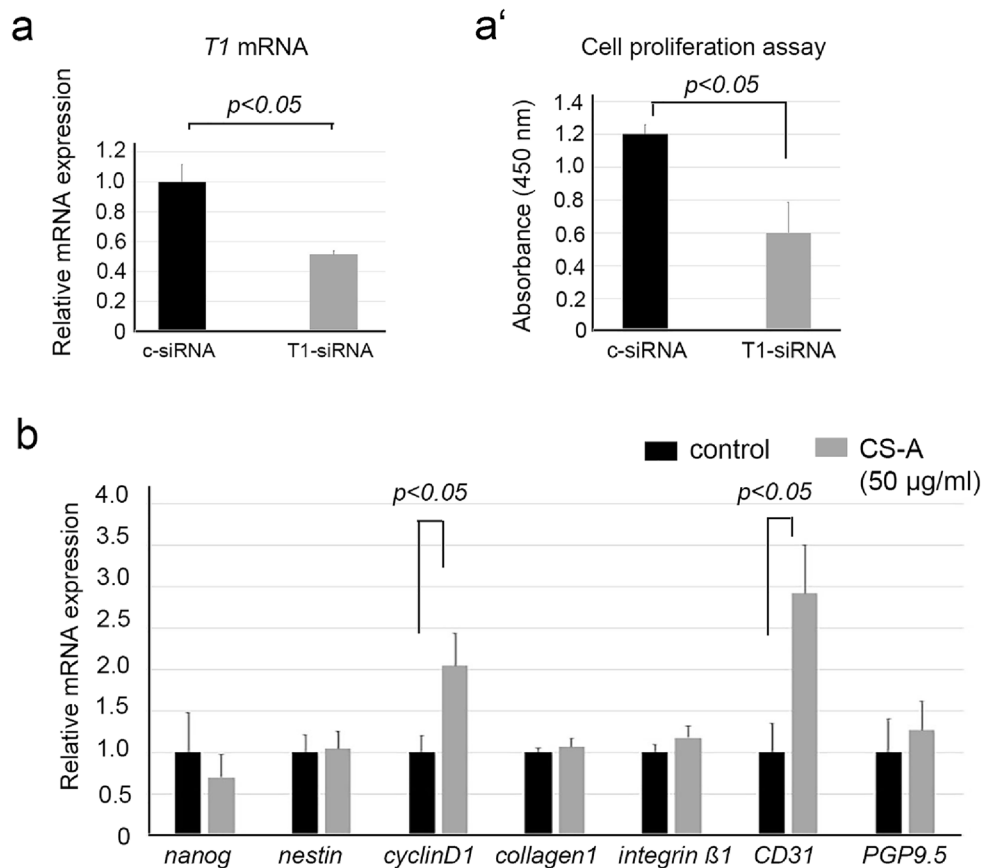
Fig. 7 Effect of T1 gene knockdown and external CS on dental pulp cells in vitro. (**a, a'**) T1 siRNA experiment in primary dental pulp cells of WT molars. T1 mRNA expression is significantly downregulated by siRNA, and cell proliferation is significantly inhibited by *T1* gene knockdown in CCK-8 assay. n = 10 for each. (**b**) T1KO dental pulp cells are cultivated on the recombinant CS-A-coated dish (50 µg/mL) for 48 h. The mRNA expressions of *cyclin D1* and *CD31* are significantly upregulated by extracellular CS. n = 6 for each, Student's *t* test

et al. 2017) will lead to the answer for the function of CS in dentinogenesis.

In relation to angiogenesis and PGs, it is well known that HS promotes blood vessel formation by interacting with several angiogenic factors, such as vascular endothelial growth factors (VEGF) and FGF2 (van Wijk and van Kuppevelt, 2014). On the other hand, CS is reported to have both pro-angiogenic and anti-angiogenic effects depending on the tissue (Le Jan et al. 2012; Kastana et al. 2019; Palhares et al. 2020). CS can bind to pro-angiogenic factors, such as VEGF-A and TGF-ß, and induce vessel maturation and angiogenesis (Le Jan et al. 2012; Souza Lins Borba et al. 2017). Regarding anti-angiogenic action, CS inhibits endothelial cell adhesion and tube formation in vitro (Kobayashi et al. 2017). In the early regeneration process of the dental pulp, CS colocalized with proliferating CD31-positive cells in the periapical region (Fig. 2h). In addition, the cell proliferation of endothelial cells and pericytes was decreased in the T1KO dental pulp (Fig. 5a–l). In vitro, the mRNA expression of CD31 was significantly upregulated by external CS in the T1KO primary dental pulp cells (Fig. 7b), suggesting that CD31-positive endothelial progenitor cells are activated by extracellular CS. Taken together, we speculate that CS might act as pro-angiogenic matrices in the early developmental and healing process of dental pulp.

In conclusion, CS is involved in the cell proliferation of dental pulp cells, including vascular cells, and supports odontoblast differentiation and functional maturation to form dentin matrices in the developmental and healing process of the dental pulp. In the developed teeth, CS may act as stem cell niche to maintain the dental pulp stem cells in the apical papilla and perivascular lesions. Therefore, CS might be available for use as a new modulator for the regeneration of dentin–pulp complex in dental tissue engineering.

Declarations

References

Ashworth S, Harrington J, Hammond GM, Bains KK, Koudouna E, Hayes AJ, Ralphs JR, Regini JW, Young RD, Hayashi R, Nishida K, Hughes CE, Quantock AJ (2020) Chondroitin Sulfate as a Potential Modulator of the Stem Cell Niche in Cornea. Front Cell Dev Biol 8:567358

Bouvier M, Joffre A, Magloire H (1990) In vitro mineralization of a three-dimensional collagen matrix by human dental pulp cells in the presence of chondroitin sulphate. Arch Oral Biol 35:301–309

Canning DR, Brelsford NR, Lovett NW (2016) Chondroitin sulfate effects on neural stem cell differentiation. In Vitro Cell Dev Biol Anim 52:35–44

Dorvee JR, Gerkowicz L, Bahmanyar S, Deymier-Black A, Veis A (2016) Chondroitin sulfate is involved in the hypercalcification of the organic matrix of bovine peritubular dentin. Arch Oral Biol 62:93–100

Embery G, Hall R, Waddington R, Septier D, Goldberg M (2001) Proteoglycans in dentinogenesis. Crit Rev Oral Biol Med 12:331–349

Galindo LT, Mundim M, Pinto AS, Chiarantin GMD, Almeida MES, Lamers ML, Horwitz AR, Santos MF, Porcionatto M (2018) Chondroitin Sulfate Impairs Neural Stem Cell Migration Through ROCK Activation. Mol Neurobiol 55:3185–3195

Ida-Yonemochi H, Morita W, Sugiura N, Kawakami R, Morioka Y, Takeuchi Y, Sato T, Shibata S, Watanabe H, Imamura T, Igarashi M, Ohshima H, Takeuchi K (2018) Craniofacial abnormality with skeletal dysplasia in mice lacking chondroitin sulfate N-acetylgalactosaminyltransferase-1. Sci Rep 8:17134

Ida-Yonemochi H, Nakajima M, Saku T (2010) Heparanase, heparan sulfate and perlecan distribution along with the vascular penetration during stellate reticulum retraction in the mouse enamel organ. Arch Oral Biol 55:778–787

Ida-Yonemochi H, Ohshiro K, Swelam W, Metwaly H, Saku T (2005) Perlecan, a basement membrane-type heparan sulfate proteoglycan, in the enamel organ: its intraepithelial localization in the stellate reticulum. J Histochem Cytochem 53:763–772

Ida-Yonemochi H, Otsu K, Ohshima H, Harada H (2016) The glycogen metabolism via Akt signaling is important for the secretion of enamel matrix in tooth development. Mech Dev 139:18–30

Igarashi M, Takeuchi K, Sugiyama S (2018) Roles of CSGalNAcT1, a key enzyme in regulation of CS synthesis, in neuronal regeneration and plasticity. Neurochem Int 119:77–83

Kastana P, Choleva E, Poimenidi E, Karamanos N, Sugahara K, Papadimitriou E (2019) Insight into the role of chondroitin sulfate E in angiogenesis. Febs j 286:2921–2936

Khadiza N, Hasegawa T, Nagai T, Yamamoto T, Miyamoto-Takasaki Y, Hongo H, Abe M, Haraguchi M, Yamamoto T, Yimin QZ, Sasaki M, Kuroshima S, Ohshima H, Freitas PHL, Li M, Yawaka Y, Amizuka N (2019) Immunolocalization of podoplanin/E11/gp38,

CD44, and endomucin in the odontoblastic cell layer of murine tooth germs. Biomed Res 40:133–143

Kobayashi T, Kakizaki I, Nozaka H, Nakamura T (2017) Chondroitin sulfate proteoglycans from salmon nasal cartilage inhibit angiogenesis. Biochem Biophys Rep 9:72–78

Le Jan S, Hayashi M, Kasza Z, Eriksson I, Bishop JR, Weibrecht I, Heldin J, Holmborn K, Jakobsson L, Söderberg O, Spillmann D, Esko JD, Claesson-Welsh L, Kjellén L, Kreuger J (2012) Functional overlap between chondroitin and heparan sulfate proteoglycans during VEGF-induced sprouting angiogenesis. Arterioscler Thromb Vasc Biol 32:1255–1263

Lei T, Zhang X, Du H (2021) Characteristics, Classification, and Application of Stem Cells Derived from Human Teeth. Stem Cells Int 2021:8886854

Listik E, Azevedo Marques Gaschler J, Matias M, Neuppmann Feres MF, Toma L, Raphaelli Nahás-Scocate AC (2019) Proteoglycans and dental biology: the first review. Carbohydr Polym 225:115199

Liu L, Chen W, Li L, Xu F, Jiang B (2017) Inhibition of chondroitin sulfate glycosaminoglycans incorporation affected odontoblast differentiation in cultured embryonic mouse molars. J Mol Histol 48:337–345

Mizumoto S, Yamada S, Sugahara K (2015) Molecular interactions between chondroitin-dermatan sulfate and growth factors/receptors/matrix proteins. Curr Opin Struct Biol 34:35–42

Murakami Masuda Y, Wang X, Yokose S, Yamada Y, Kimura Y, Okano T, Matsumoto K (2010) Effect of glypican-1 gene on the pulp cells during the reparative dentine process. Cell Biol Int 34:1069–1074

Nadanaka S, Kinouchi H, Taniguchi-Morita K, Tamura J, Kitagawa H (2011) Down-regulation of chondroitin 4-O-sulfotransferase-1 by Wnt signaling triggers diffusion of Wnt-3a. J Biol Chem 286:4199–4208

Nakatomi M, Quispe-Salcedo A, Sakaguchi M, Ida-Yonemochi H, Okano H, Ohshima H (2018) Nestin expression is differently regulated between odontoblasts and the subodontoblastic layer in mice. Histochem Cell Biol 149:383–391

Nishimura K, Ishii M, Kuraoka M, Kamimura K, Maeda N (2010) Opposing functions of chondroitin sulfate and heparan sulfate during early neuronal polarization. Neuroscience 169:1535–1547

Palhares L, Barbosa JS, Scortecci KC, Rocha HAO, Brito AS, Chavante SF (2020) In vitro antitumor and anti-angiogenic activities of a shrimp chondroitin sulfate. Int J Biol Macromol 162:1153–1165

Prinz RD, Willis CM, van Kuppevelt TH, Klüppel M (2014) Biphasic role of chondroitin sulfate in cardiac differentiation of embryonic stem cells through inhibition of Wnt/β-catenin signaling. PLoS One 9:e92381

Randilini A, Fujikawa K, Shibata S (2020) Expression, localization and synthesis of small leucine-rich proteoglycans in developing mouse molar tooth germ. Eur J Histochem 64:

Saito K, Ohshima H (2017) Differentiation capacity and maintenance of dental pulp stem/progenitor cells in the process of pulpal healing following tooth injuries. J Oral Biosci 59:63–70

Shibata S, Kaneko S, Yanagishita M, Yamashita Y (1999) Histochemical localization of hyaluronan and versican in the rat molar dental pulp. Arch Oral Biol 44:373–376

Shibata S, Yoneda S, Yanagishita M, Yamashita Y (2002) Developmental changes and regional differences in histochemical localization of hyaluronan and versican in postnatal molar dental pulp. Int Endod J 35:159–165

Shimbo M, Suzuki R, Fuseya S, Sato T, Kiyohara K, Hagiwara K, Okada R, Wakui H, Tsunakawa Y, Watanabe H, Kimata K, Narimatsu H, Kudo T, Takahashi S (2017) Postnatal lethality and chondrodysplasia in mice lacking both chondroitin sulfate N-acetylgalactosaminyltransferase-1 and -2. PLoS One 12:e0190333

Sonoyama W, Liu Y, Fang D, Yamaza T, Seo BM, Zhang C, Liu H, Gronthos S, Wang CY, Wang S, Shi S (2006) Mesenchymal stem

cell-mediated functional tooth regeneration in swine. PLoS One 1:e79

Souza Lins Borba FKd, Ventura Lola Costa E, Balvedi Polli VA, Sousa Coelho D, Maraschin M, Fernando Dias P, Nogueira RA (2017) Pro-angiogenic Activity Assay of Chondroitin Sulfate and Glucosamine Sulfate on Vascular Network of Mouse and of Chick Embryo Chorioallantoic Membrane. J Glycobiol 06

Sui B, Wu D, Xiang L, Fu Y, Kou X, Shi S (2020) Dental Pulp Stem Cells: From Discovery to Clinical Application. J Endod 46:S46-s55

Takeuchi K, Yoshioka N, Higa Onaga S, Watanabe Y, Miyata S, Wada Y, Kudo C, Okada M, Ohko K, Oda K, Sato T, Yokoyama M, Matsushita N, Nakamura M, Okano H, Sakimura K, Kawano H, Kitagawa H, Igarashi M (2013) Chondroitin sulphate N-acetylgalactosaminyltransferase-1 inhibits recovery from neural injury. Nat Commun 4:2740

Uyama T, Kitagawa H, Tamura Ji J, Sugahara K (2002) Molecular cloning and expression of human chondroitin N-acetylgalactosaminyltransferase: the key enzyme for chain initiation and elongation of chondroitin/dermatan sulfate on the protein linkage region tetrasaccharide shared by heparin/heparan sulfate. J Biol Chem 277:8841–8846

Uyama T, Kitagawa H, Tanaka J, Tamura J, Ogawa T, Sugahara K (2003) Molecular cloning and expression of a second chondroitin N-acetylgalactosaminyltransferase involved in the initiation and elongation of chondroitin/dermatan sulfate. J Biol Chem 278:3072–3078

van Wijk XM, van Kuppevelt TH (2014) Heparan sulfate in angiogenesis: a target for therapy. Angiogenesis 17:443–462

Wang T, Yang F (2017) A comparative study of chondroitin sulfate and heparan sulfate for directing three-dimensional chondrogenesis of mesenchymal stem cells. Stem Cell Res Ther 8:284

Watanabe Y, Takeuchi K, Higa Onaga S, Sato M, Tsujita M, Abe M, Natsume R, Li M, Furuichi T, Saeki M, Izumikawa T, Hasegawa A, Yokoyama M, Ikegawa S, Sakimura K, Amizuka N, Kitagawa H, Igarashi M (2010) Chondroitin sulfate N-acetylgalactosaminyltransferase-1 is required for normal cartilage development. Biochem J 432:47–55

Wood CR, Al Delfi IRT, Innes JF, Myint P, Johnson WEB (2018) Exposing mesenchymal stem cells to chondroitin sulphated proteoglycans reduces their angiogenic and neuro-adhesive paracrine activity. Biochimie 155:26–36

Yang G, Ju Y, Liu S, Zhao S (2019) Lipopolysaccharide upregulates the proliferation, migration, and odontoblastic differentiation of NG2(+) cells from human dental pulp in vitro. Cell Biol Int 43:1276–1285

Zhang F, Zheng L, Cheng S, Peng Y, Fu L, Zhang X, Linhardt RJ (2019) Comparison of the interactions of different growth factors and glycosaminoglycans. Molecules 24:3360